

Estimation of Land Use Changes in Tan Rai Bauxite Mine by Multi-Variants Change Vector Analysis (MCVA) on Multi-Temporal Remote Sensing Data

Nguyen Thanh Hoan^{1,2}, Hoa Thuy Quynh¹, Le Minh Hang³, Nguyen Manh Ha^{1,2},
Hoang Thi Huyen Ngoc¹, Dang Xuan Phong^{1,2}

¹Institute of Geography, Vietnam Academy of Science and Technology, Hanoi, Vietnam

²Graduate University of Science and Technology, Vietnam Academy of Science and Technology, Hanoi, Vietnam

³Le Quy Don Technical University, Hanoi, Vietnam

Email: hoanrs@gmail.com

How to cite this paper: Hoan, N. T., Quynh, H. T., Hang, L. M., Ha, N. M., Ngoc, H. T. H., & Phong, D. X. (2020). Estimation of Land Use Changes in Tan Rai Bauxite Mine by Multi-Variants Change Vector Analysis (MCVA) on Multi-Temporal Remote Sensing Data. *Journal of Geoscience and Environment Protection*, 8, 70-84.

<https://doi.org/10.4236/gep.2020.83006>

Received: December 24, 2019

Accepted: March 28, 2020

Published: March 31, 2020

Copyright © 2020 by author(s) and Scientific Research Publishing Inc. This work is licensed under the Creative Commons Attribution International License (CC BY 4.0).

<http://creativecommons.org/licenses/by/4.0/>



Open Access

Abstract

The Tan Rai Bauxite Project, which exploits a large bauxite mine in Lam Dong province, Vietnam has been in operation since 2012. In addition to the economic efficiency of the project, bauxite mining and processing uses a large area arable land and affect the regional environment. Remote sensing technology is increasingly widely used in many purposes in monitoring the changes of environment and resources, including land use change with high accuracy, giving managers more information to monitor the exploitation and use process of land resource. This study used a Change Vector Analysis (CVA) method of analysis on various remote sensing data sources to monitor the process of land exploitation and restoration of the Tan Rai Bauxite project. High-resolution remote sensing images were used as diverse as SPOT-5, VNREDSat-1, Google Earth from 2013 to 2019 to demonstrate the ability of the MCVA method to combine many other types of remote sensing images together. The results of fluctuation analysis were validated by 200 random points in the study area, and the accuracy of result is more than 90%. The results of land use change statistics were also compared with the annual data of Tan Rai Bauxite Factory. From this study, it can be concluded that the MCVA analysis method can quickly detect land use change areas and can combine many different image sources with a high accuracy. In addition, it also provides statistics of mining areas and restored areas, thereby assisting managers in monitoring the operation of the mine.

Keywords

Bauxite Tan Rai, MCVA, Land Use Change, Monitoring, Multi-Sensors

1. Introduction

The Central Highlands of Vietnam is a highland area which includes in 5 provinces (Kon Tum, Gia Lai, Dak Lak, Dak Nong and Lam Dong) with approximately 16.8% of the country's natural area. It has diverse and rich mineral resources with large reserves included in peat, brown coal, kaolin clay and some heavy metals, bauxite and iron.... Tan Rai Bauxite Project is one of the major Bauxite mining projects in Lam Dong province that was started in 2008 and has been in operation in 2012. The total land use area for mining is more than 1600 hectares with a mining capacity about 4,318,000 tons annually. Unfortunately, the bauxite processing and mining over the years has affected the regional environment as well as changing of land cover. The leveling, building factories caused to fluctuation the landscape, reduce the ecosystem or pollute water resources by the discharge from the operation of these factories. Hence, it is necessary to find a method for monitoring and observing land cover changes by the operation of bauxite mine. According to that it helps the managers to support the efficient and sustainable solutions for using natural resources.

The development of space technology, typically artificial satellites, has created a new era for monitoring land cover changes in wide area with fast updating and quite high accuracy. Based on remote sensing data, we can interpret, analyze and evaluate the fluctuations of land cover in time. SPOT-5, VNREDSat-1 satellite images with 5 m spatial resolution have the advantages for monitoring land cover types of a regional-scale.

Many researches about the monitoring fluctuations of land cover have been studied. The first global land cover map by using satellite data was IGBP DIS-Cover using 1 km AVHRR data in 1992 (Loveland, Reed, Brown, Ohlen, Zhu, Yang et al., 2000). Subsequently, global land cover maps were created by the University of Maryland in USA using the AVHRR data of NOAA satellite (Hansen, Defries, Townshend, & Sohlberg, 2000), Boston University using the 1 km MODIS data in 2002 (Friedl, McIver, Hodges, Zhang, Muchoney, Strahler et al., 2002). In 2005, the European space agency (ESA) established the GLOBCover Land cover using MERIS data with 300m spatial resolution (Arino, Gross, Ranera, Bourg, Leroy, Bicheron et al., 2007). Chiba University in Japan, which had the cooperation with a number of the organizations, developed GLCNMO (The Global Land Cover by National Mapping Organizations) version 1 using MODIS 1 km data (Tateishi, Uriyangqai, Al-Bilbisi, & Ghar, 2011) in 2003. The GLCNMO version 2 were built in 2008 by using MODIS 500 m data (Tateishi, Hoan, Kobayashi & Alsaaidh, 2014) and the GLCNMO version 3 in 2013 by using MODIS 500 m data (Kobayashi, Tateishi, Alsaaidh, Sharma, Wakaizumi, Miyamoto et al., 2017). However, the accuracy of these global land cover maps were only

around 80%, which were unsuitable for detecting and creating the fluctuation maps with the purpose of environmental observation and natural resource management (Bayan, Hoan, & Tateishi, 2014).

The method of detecting land cover changes was based on the comparison of classification results in two periods. The satellite data are commonly used such as Landsat images and SPOT5 images (Butt, Shabbir, Ahmad, & Aziz, 2015; Abdullah, Masrur, Adnan, Baky, Hassan, & Dewan, 2019). Nowadays, the spectral reflectance index of land cover objects is applied for improving high classification accuracy. For examples, the snow cover were determined by analysis the spectral reflectance indexes of satellite data (Crane & Anderson, 1984; Rosenthal, & Dozier, 1996; Hall, Riggs, Salomonson, Girolamo, & Bayr, 2002; Salomonson & Appel, 2004; Painter, Rittger, McKenzie, Slaughter, Davis, & Dozier, 2009). To distinguish between waters and snow, (Sharma, Tateishi, & Hara, 2016) has developed water-resistant snow index (WSI). In order to detect urban and water areas, the Normalized Difference Water Index (NDWI) (McFeeters, 1996; Gao, 1996) and the Normal Difference Built-up Index (NDBI) (Zha, Gao & Ni, 2003; Sharma, Tateishi, Hara, Gharechelou, & Lizuka, 2016) were built. The barren land index has developed by many researchers (Rogers & Kearney, 2004; Deng, Wu, Li, & Chen, 2015; Sharma, Tateishi, & Hara, 2016). The Enhanced Vegetation Index (EVI) and Normalized difference vegetation index (NDVI) were used to classify cultivated areas by MODIS data (Brian, Stephen, & Jude, 2007). Besides, (Haque & Basak, 2017) used Maximum likelihood classification method which the input data were NDVI and NDWI images of Landsat data and used Change Vector Analysis (CVA) to determine the land cover changes in Tanguar Haor, Bangladesh. Most studies have achieved an accepted accuracy. But they have been tested only in wide area by medium resolution of remote sensing data. In this study, we would like to emphasize the importance of input variables for the use of change vector analysis method. In particular, input variables are decided mainly based on subjective opinions of experts from image analysis experience. These variables are the crystallization of image analysis experiences of experts and the name of the CVA method was changed to Multi-variant Change Vector Analysis (MCVA). MCVA method bases on the expert knowledge to combine the spectral reflectance indexes and potential variables to achieve the highest efficiency (Johnson & Kasischke, 1998; Nackaerts, Vaesen, Muys, & Coppin, 2005; Jin, Xuehong, Xihong & Jun, 2010). In this article, we assessed the ability and effectiveness of using high-resolution remote sensing data to determine the land cover changes based on the analysis of multivariate vector and the comparison the fluctuations indicators between different periods of time, a case study in Bauxite Tan Rai mine in Lam Dong province, Vietnam.

2. Study Area and Materials

2.1. Study Area

Bauxite Tan Rai mine is located in the wards of Loc Thang, Loc Phu and Loc

Ngai of Bao Lam district in Lam Dong province. The total area of Tan Rai mine is more than 1600 hectares (**Figure 1**).

The study area includes in the entire mining area, factory ground area and the area around the mine. Tan Rai mine is located in the East of Bao Loc-Di Linh plateau. The plateau terrain is relatively flat, inclined from the Northeast to the Southwest. The annual average temperature is 21.7°C with the total annual rainfall of 2356.5 mm. The mine area is largely covered by double-leaved pine forests intercropped with industrial trees such as coffee and tea. The population of Bao Lam district in Tan Rai mine was 100,000 people with a population density of about $66\text{ people}/\text{km}^2$ and distributed along both sides of provincial roads, mainly living in Loc Thang town.

2.2. Materials

In order to the requirements of monitoring the land cover changes in a regional scale with not large area, the experience materials were SPOT5, Google Earth and VNREDSat-1 images. The characteristics of the satellite data were shown in **Table 1**.

Fusion multispectral bands and panchromatic band of VNREDSat-1 data was created. The satellite images were re-projected to VN2000 coordinate system and 2.5m spatial resolution.

3. Methodology and Results

3.1. Multi-Variant Change Vector Analysis (MCVA)

Multi-variant Change Vector Analysis (MCVA) is used to detect land cover changes based on change vector components. The MCVA is the method which uses expert knowledge and combines with indexes and variables to attend the

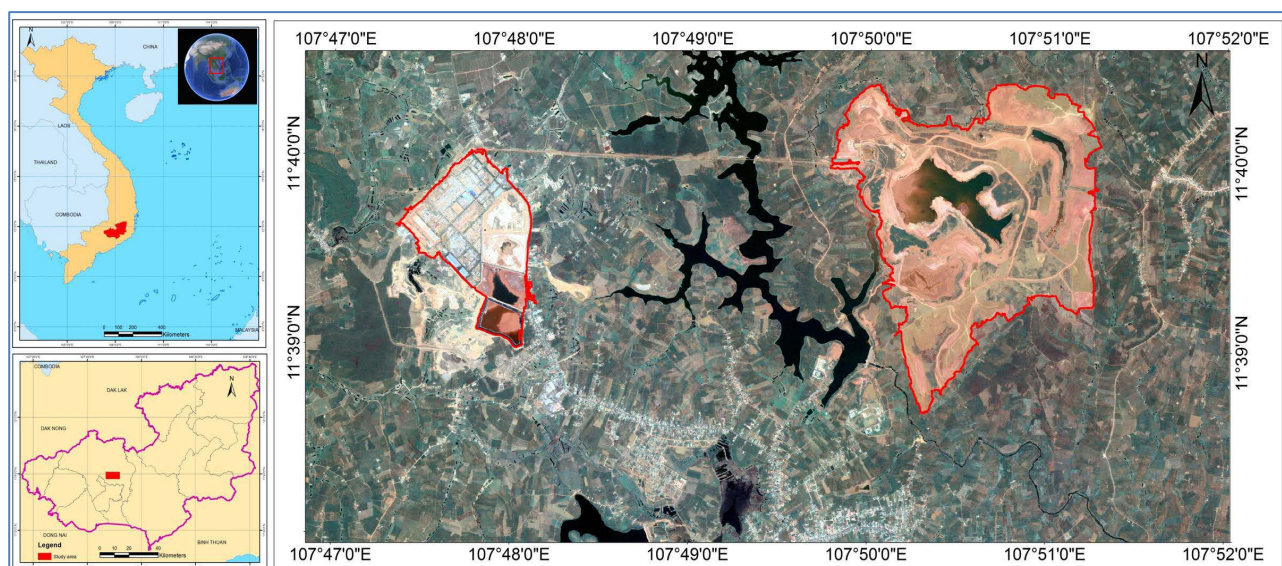


Figure 1. Study area (red polygons): (a) Location of Vietnam; (b) Position of Tan Rai bauxite mine in Lam Dong province; (c) Tan Rai bauxite mine in VNRedSAT image (2018).

Table 1. The characteristics of the experience materials.

No	Sensors	Date	Level	Coordinates	Resolution
1	SPOT5	15/4/2013	3A	VN2000	2.5 m
	Google Earth	16/2/2014		WGS84	2.5 m
2		09/5/2016		WGS84	2.5 m
		16/3/2019		WGS84	2.5 m
3	VNREDSat-1	16/2/2015	3A	VN2000	2.5 m
		03/1/2018		VN2000	2.5 m

purposes (Johnson & Kasischke, 1998; Jin, Xuehong, Xihong, & Jun, 2010). The objective of this study is to propose a method that can analyze very high-resolution images but that have no original spectral values such as Google Earth, SPOT 5-6-7, VNRedsat-1 after pan-sharpen process. These types of images are often processed pan-sharpen to keep true color composite. That means, on these processed images, the plants will be green color, the soil will be brown color (red + blue) and the water will be blue color. According to logical analysis, if plants are lost, the green color of the area will be decreased; If the percentage covered by bare land increases then the red and blue color will be increased.

In this study, we proposed to three indexes such as GB, RG and RB based on expert analysis. Three indexes were converted to 8-bit color. The equations of three indexes were as following:

$$GB = \frac{G - B}{G + B} * 127 + 128 \quad (1)$$

$$RG = \frac{R - G}{R + G} * 127 + 128 \quad (2)$$

$$RB = \frac{R - B}{R + B} * 127 + 128 \quad (3)$$

where: R —Spectral reflectance of Red band;

G —Spectral reflectance of Green band;

B —Spectral reflectance of Blue band.

These indexes were proposed by the characteristics of spectral reflectance of land cover objects. The plants reflect strongly by green band. As a result, if the plants are removed, the value of green band on satellite images will decrease. Similarly, the soil reflects by red band or blue band which depends on the physical characteristics of the soil. Therefore, when plants are removed, the spectral reflectance value of the red and blue band increases and the values of green band decrease. The MCVA method is based on dimensional analysis vector changes of GB , RG and RB index variables.

Vector change of GB index is defined as following:

$$VC_{GB} = GB(1) - GB(2) \quad (4)$$

Vector change of RG index is defined as following:

$$VC_{RG} = RG(2) - RG(1) \quad (5)$$

Vector change of *RB* index is defined as following:

$$VC_{RB} = RB(2) - RB(1) \quad (6)$$

where: 1) the value of the previous time and 2) the value of the later time.

According to logical analysis, if plants are lost, the value of *GB* index will decrease and vector change of *GB* index is positive. In this case, the value of *RG* and *RB* indexes will increase and vector change of these indexes is positive. As a result, the total vector change is defined by the following equation:

$$\text{ChangeIndex1} = \sqrt{VC_{GB}^2 + VC_{RG}^2 + VC_{RB}^2} \quad (7)$$

where: *GB*(1), *RG*(1), *RB*(1)—The value of *GB*, *RG*, *RB* index in the previous time;

GB(2), *RG*(2), *RB*(2)—The value of *GB*, *RG*, *RB* index in the later time.

However, there are algae and chlorophyll in water which reflect green band and absorb red band. In order to reduce the misclassification because of water fluctuation confusion, we proposed to use NGRDI (Normalized Green-Red difference index) (Tucker, 1979; Gitelson, Kaufman, Stark, & Rundquist, 2002) to distinguish water surface. NGRDI index is calculated as follows:

$$\text{NGRDI} = \frac{G - R}{G + R} \quad (8)$$

where: *R*—Spectral reflectance of Red band;

G—Spectral reflectance of Green band.

Firstly, Change Index 1 image was segmented by the Multi-resolution Segmentation algorithm in Ecognition software. Secondly, the mean value and the standard deviation of each segment were calculated. The changes of land cover were classified based on the threshold of mean value of each segment in Change Index 1 image.

The accuracy of change detection is identified by evaluating the performance of each potential threshold which is used to classify change/no-change segments. The accuracy (*D*) is calculated by the equation as follows:

$$D(\%) = \frac{a}{b} \times 100\% \quad (9)$$

where: *D*(%)—The accuracy of change detection; *a*—The number of training patches in ChangeIndex1 image which are identified land cover changes; *b*—The number of the sample points in a map for evaluating the results.

In this article, we selected 100 random change points and 100 random no-change points in a pair of images to evaluate the results.

3.2. Classification Results and Discussion

3.2.1. Estimating the Changes of Land Cover in Tan Rai Bauxite Mine

The order of exploiting bauxite in Tan Rai has 5 main steps: 1) clearing the surface; 2) opening the seams; 3) peeling off the covered soil layer by scrapping along the slope direction or transporting at the landfill awaiting restoration; 4) extracting ore in order from the outside inward for the top and from top to bot-

tom for the ribs and 5) finally restoration. This process changed the regional land cover in general as well as affecting the living environment of people.

1) Using SPOT5 from 2013 to 2016

The segmentation results of Change Index image of SPOT5 in the bauxite area of Tan Rai in the period of 2013-2016 included 53,902 segments. The boundary of these segments was illustrated in **Figure 2**.

To detect land cover changes, we calculated the mean value of each segment of the Change Index 1 and NRGDI image. After that, we selected a potential threshold with the ability of land cover changes such as “Change Index” ≥ 40 AND “NRGDI” ≤ 0.07 AND “areas” ≥ 500 (**Figure 3**).

Bauxite ore refining factory discharged waste sludge products in the process. After being concentrated, the sludge of the concentrate tank is pumped to the tailings sludge dumps. Changes of sludge lakes or changes of water quality were also detected by Change Index 1 index (**Figure 4**).

100 random points in changed areas and 100 random points in no-changed areas were selected in the whole image for validation (**Figure 5**). In the mining area, in 37 checked points, there were 35 points which were detected by Change Index. So the accuracy is 94.5%. The accuracy of no-change detection was 100% accuracy.

2) Using GE image from 2014 to 2016

We applied the same method for Google Earth images during 2014-2016. The potential threshold with the ability of changes land cover in ChangeIndex1 and



Figure 2. The segmentation results in SPOT5 images.

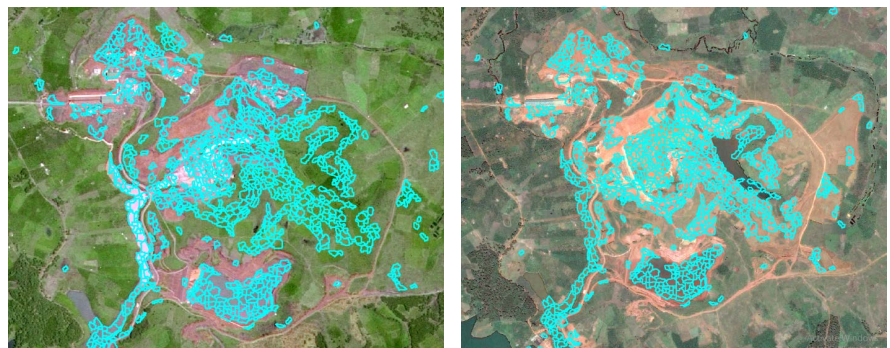


Figure 3. The land cover changes result using change index image of SPOT5.



Figure 4. The location of the sludge lake has a change in water quality in SPOT5.

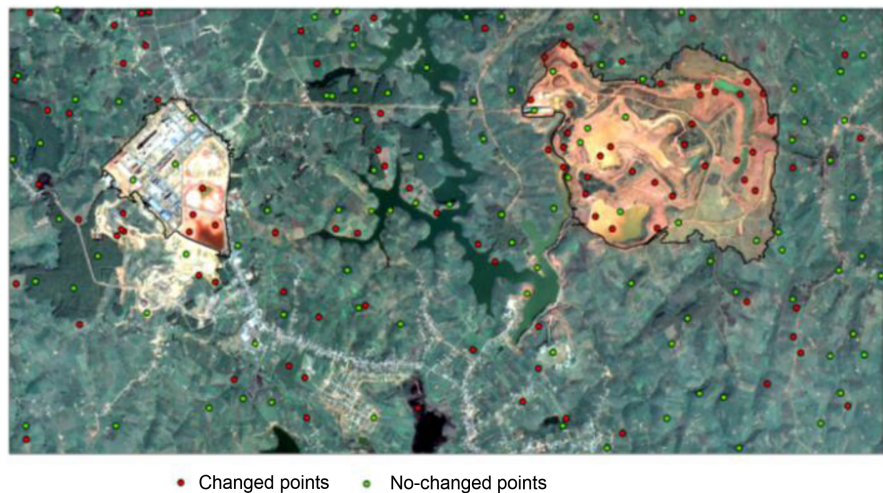


Figure 5. The location of validation points.

NRGDI of Google Earth image such as “Change Index” ≥ 40 AND “NRGDI” ≤ 0.07 AND “areas” ≥ 500 (**Figure 6**).

In the mining area, there were 37 correct points in 40 checked points. The reference accuracy archived 92.5%. The accuracy of no-change detection was 100% accuracy.

3) Using VNRedSAT images from 2015 to 2018

The potential threshold with the ability of changes land cover in Change Index and NRGDI of GE image such as “Change Index” ≥ 30 and “NRGDI” ≤ 0.07 AND “areas” ≥ 500 . The classification results by using VNRedSAT images from 2015 to 2018 are shown in **Figure 7** and **Figure 8**.

In the mining area, there were 35 correct points in 36 checked points. The reference accuracy archived 97.2%. The accuracy of no-change detection was 100% accuracy.

3.2.2. Land Cover Maps of Tan Rai Bauxite Area in 2013, 2015, 2018, 2019

The land cover map of Bauxite Tan Rai area in 2013, 2015, 2018 and 2019 are shown in **Figures 9(a)-(d)**, respectively. The five main types of land cover include vegetation, bare land, crop land, water and other lands. According to

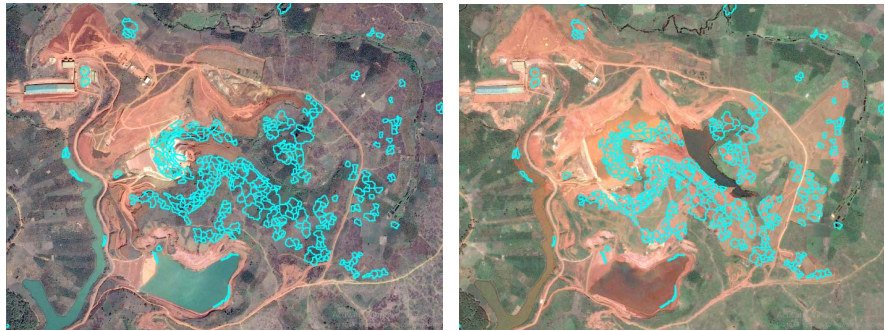


Figure 6. The segments of land cover changes in GE images.

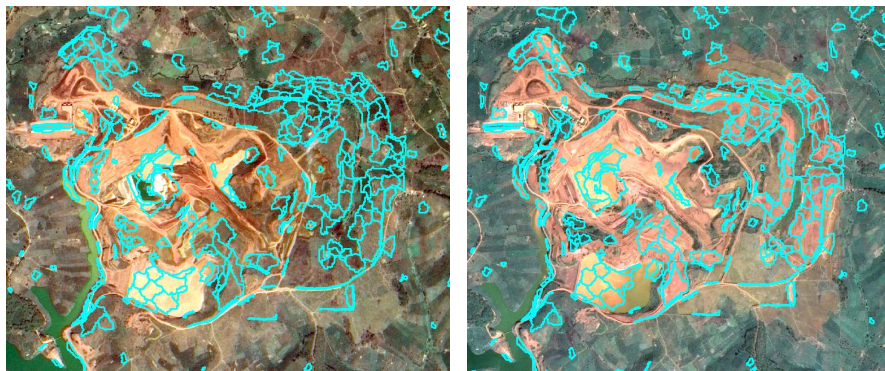


Figure 7. The segments of land cover changes in VNRedSAT images.



Figure 8. The location of the sludge lake has a change in water quality.

analysis the land cover maps of Bauxite Tan Rai mine over the years, we can see that the mine area has been expanded over time and increased dramatically. The most of mining area was transferred of land use from cropland to bare land and sludge lakes (water surface). In addition, a number of the areas after mining process have been restored from bare land to vegetation.

To assess the accuracy of land cover classification, we used 150 random points, which were clearly identified on Google Earth and Google Map. The overall accuracy of classification results in 2013 reached 95.3%, in 2015 reached 92.6%, in 2018 reached 94.6% and in 2019 reached 96.6%. The accuracy

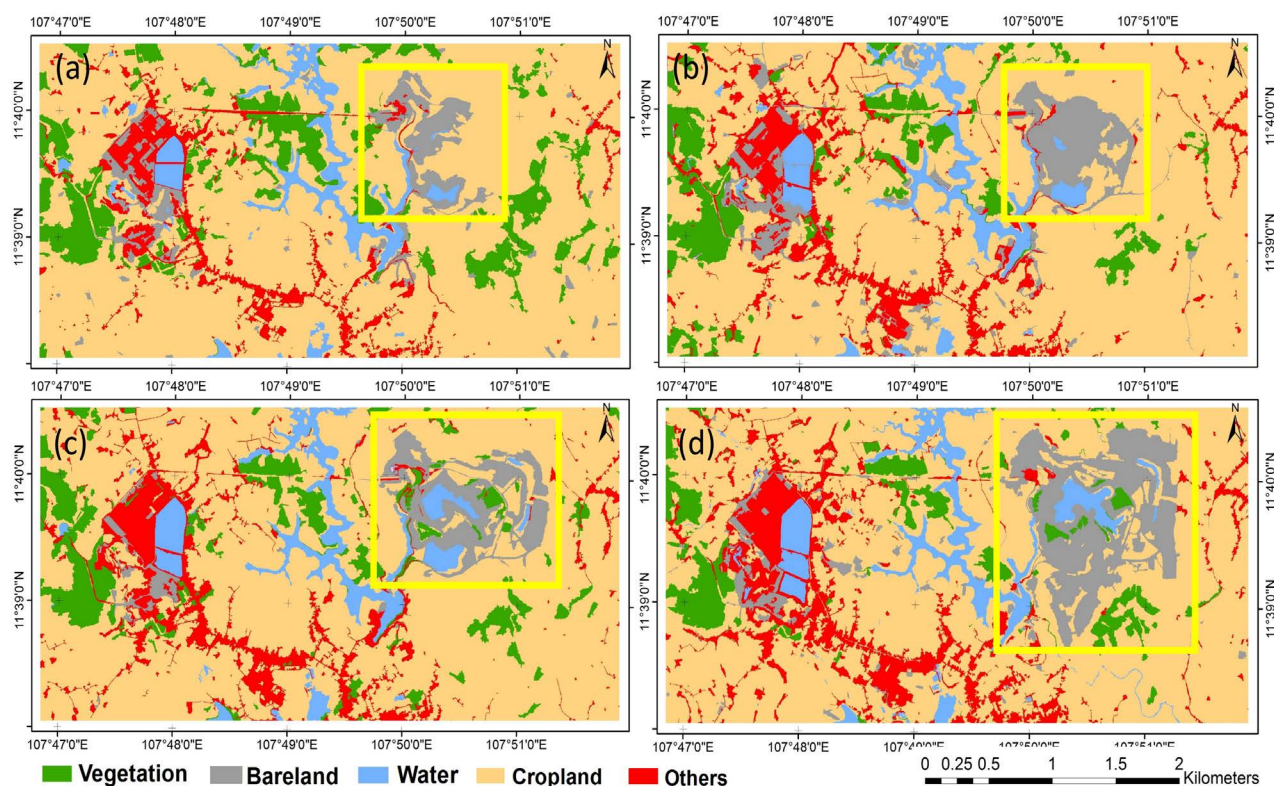


Figure 9. Land cover maps of bauxite Tan Rai area. (a) In 2013; (b) In 2015; (c) In 2018; (d) In 2019.

assessment is shown in the confusion matrix in **Tables 2-5** as following.

3.2.3. Assessment the Land Cover Change in Bauxite Tan Rai Area during Period 2013-2019

Lam Dong aluminum bauxite complex project was approved in 2006, officially started construction of Alumina Factory in 2008 and completed the commissioning and officially put into operation in 2013. It is expected that bauxite ore will be 4,318,000 tons/year, refined ore will be 1,775,000 tons/year and production and commercial capacity will be 630,000 tons of alumina/year. In addition to expanding the mining area over many years, the project also conducted to restore the regional land cover in accordance with the regulations after the exploitation. After dumping, all landfill sites must be leveled and covered with soil, vegetation or applied a suitable method with the characteristics of region.

Based on the segmentation results of Change Index 1 image, we can calculate the Tan Rai mining area and the restoration area over each period (**Figure 10**).

The statistics of area results which calculated by satellite images and the 2013-2019 report are shown in **Table 6**.

According to the statistical results, the mining area tended to increase over time and increased rapidly over the past year. The results of the exploitation area and the restoration area calculated by using satellite images are quite similar with local reports. The error may be due to the synchronization of the acquisition date of satellite image and the statistical report.

Table 2. The confusion matrix of classification result in 2013 by using SPOT5.

Classified	Reference Data				
	Others	Cropland	Bareland	Water	Vegetation
1 Others	16	1	0	0	0
2 Cropland	0	94	0	0	4
3 Bareland	0	0	11	0	0
4 Water	0	0	0	6	0
5 Vegetation	0	2	0	0	16
Overall accuracy: 95.3%					

Table 3. The confusion matrix of classification result in 2015 by using VNREDSat-1.

Classified	Reference Data				
	Others	Cropland	Bareland	Water	Vegetation
1 Others	15	1	1	0	0
2 Cropland	4	92	2	2	0
3 Bareland	0	1	16	0	0
4 Water	0	0	0	6	0
5 Vegetation	0	0	0	0	10
Overall Accuracy: 92.6%					

Table 4. The confusion matrix of classification result in 2018 by using VNRedSAT.

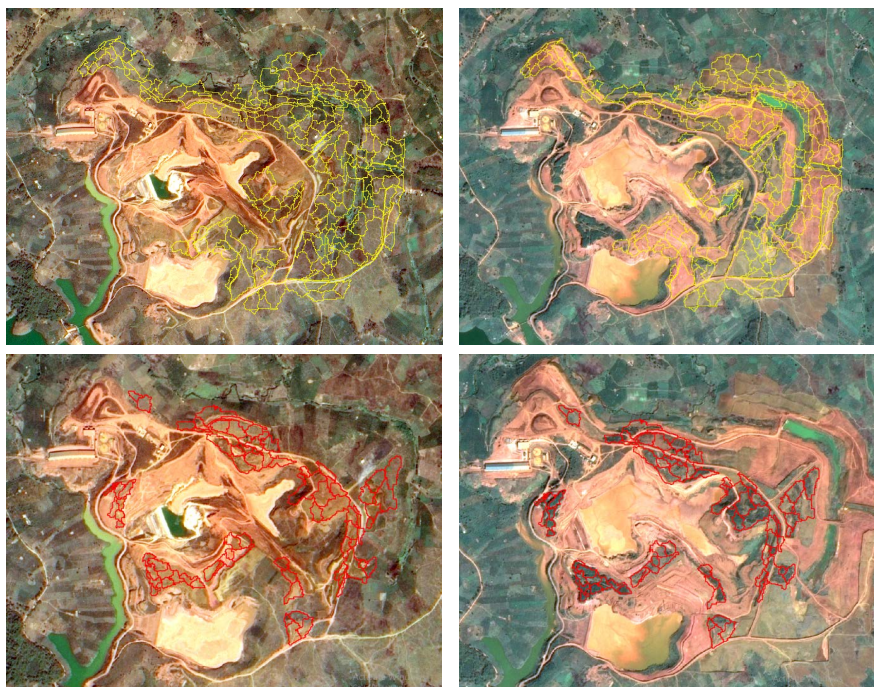
Classified	Reference Data				
	Others	Cropland	Bareland	Water	Vegetation
1 Others	14	3	0	0	0
2 Cropland	1	94	0	0	3
3 Bareland	0	0	18	0	0
4 Water	0	0	0	7	0
5 Vegetation	0	1	0	0	9
Overall Accuracy: 94.6%					

Table 5. The confusion matrix of classification result in 2019 by using Google Earth.

Classified	Reference Data				
	Others	Cropland	Bareland	Water	Vegetation
1 Others	17	0	0	0	0
2 Cropland	0	97	0	0	1
3 Bareland	1	1	17	0	0
4 Water	0	0	0	7	0
5 Vegetation	0	2	0	0	7
Overall Accuracy: 96.6%					

Table 6. The statistics of exploitation and restoration areas during 2013-2019.

Years	2015-2018	2018-2019	2013-2019
Area Exploitation (ha) (Satellite Images)	182.697	71.9	259.99
Area Exploitation (ha) (Report)	188.69	70.18	258.87
Area Restoration (ha) (Satellite Images)	46.44	35.15	103.56
Area Restoration (ha) (Report)	47.62	35.67	116.78

**Figure 10.** Delineate the mining area (yellow polygons - upper images) and the restoration areas (red polygons - lower images) in period 2015 (left) - 2018 (right).

4. Conclusion

In conclusion, MCVA method can quickly identify land cover changes in high resolution satellite image. The change vectors were proposed by the spectral reflectance of satellite bands in two times. In addition, the water quality change areas were also detected by the change vector analysis. In this article, we used the object-based to detect the change/no-change objects in Change Index 1 image. According to the classification result, the potential threshold for detecting land cover changes in Change Index images are different in each type of satellite images. The classification accuracy of the inner mining areas is higher than the around area.

MCVA method can detect and determine the land cover areas during bauxite mining operation such as expanded mining area, restoration area and reforestation, etc. According to that, it helps to support the solutions to improve and restore the environment after the end of exploitation.

The Bauxite Tan Rai area is quite small, but the proposed method in this study has achieved high accuracy. Recently, Google Earth images are free of charge, high spatial resolution and regular updates so that the proposed method can be applied Google Earth images to monitor the land cover changes of the mineral mines during the mining operation in Vietnam.

Acknowledgements

This research was funded by Tay Nguyen Program 2016-2020 under project codes: TN17/T04, TN18/T10 and Vietnam Academy of Science and Technology (VAST) under project codes: KHCBTĐ.02/19-21, UQĐTCB.02/19-20.

Conflicts of Interest

The authors declare no conflicts of interest regarding the publication of this paper.

References

- Abdullah, A. Y. M., Masrur, A., Adnan, M. S. G., Baky, M. A. A., Hassan, Q. K., & Dewan, A. (2019). Spatio-Temporal Patterns of Land Use/Land Cover Change in the Heterogeneous Coastal Region of Bangladesh between 1990 and 2017. *Remote Sensing*, *11*, 790. <https://doi.org/10.3390/rs11070790>
- Arino, O., Gross, D., Ranera, F., Bourg, L., Leroy, M., Bicheron, P. et al. (2007). GLOBCover: ESA service for Global Land Cover from MERIS. In *International Geoscience and Remote Sensing Symposium (IGARSS)* (pp. 2412-2415). <https://doi.org/10.1109/IGARSS.2007.4423328>
- Bayan, A., Hoan, N. T., & Tateishi, R. (2014). Comparison and Validation of Five Global Land Cover Products. In *Proceedings of International Symposium on Remote Sensing 2014 (ISRS 2014)* (pp. 65-68). Busan, Korea.
- Brian, D. W., Stephen, L. E., & Jude, H. K. (2007). Analysis of Time-Series MODIS 250 m Vegetation Index Data for Crop Classification in the U.S. Central Great Plains. *Remote Sensing of Environment*, *108*, 290-310. <https://doi.org/10.1016/j.rse.2006.11.021>
- Butt, A., Shabbir, R., Ahmad, S. S., & Aziz, N. (2015). Landuse Change Mapping and Analysis Using Remote Sensing and GIS: A Case Study of Simply Watershed, Islamabad, Pakistan. *The Egyptian Journal of Remote Sensing and Space Sciences*, *18*, 251-259. <https://doi.org/10.1016/j.ejrs.2015.07.003>
- Crane, R. G., & Anderson, M. R. (1984). Satellite Discrimination of Snow/Cloud Surfaces. *International Journal of Remote Sensing*, *5*, 213-223. <https://doi.org/10.1080/01431168408948799>
- Deng, Y., Wu, C., Li, M., & Chen, R. (2015). RNDSI: A Ratio Normalized Difference Soil Index for Remote Sensing of Urban/Suburban Environments. *International Journal of Applied Earth Observation and Geoinformation*, *39*, 40-48. <https://doi.org/10.1016/j.jag.2015.02.010>
- Friedl, M.A., McIver, D. K., Hodges, J. C. F., Zhang, X. Y., Muchoney, D., Strahler, A.H. et al. (2002). Global Land Cover Mapping from MODIS: Algorithms and Early Results. *Remote Sensing of Environment*, *83*, 287-302. [https://doi.org/10.1016/S0034-4257\(02\)00078-0](https://doi.org/10.1016/S0034-4257(02)00078-0)
- Gao, B. (1996). NDWI: A Normalized Difference Water Index for Remote Sensing of

- Vegetation Liquid Water from Space. *Remote Sensing of Environment*, 58, 257-266. [https://doi.org/10.1016/S0034-4257\(96\)00067-3](https://doi.org/10.1016/S0034-4257(96)00067-3)
- Gitelson, A. A., Kaufman, Y. J., Stark, R., & Rundquist, D. (2002). Novel Algorithms for Remote Estimation of Vegetation Fraction. *Remote Sensing of Environment*, 80, 76-87. [https://doi.org/10.1016/S0034-4257\(01\)00289-9](https://doi.org/10.1016/S0034-4257(01)00289-9)
- Hall, D. K., Riggs, G. A., Salomonson, V. V., Girolamo, N. E. D., & Bayr, K. J. (2002). MODIS Snow-Cover Products. *Remote Sensing of Environment*, 83, 181-194. [https://doi.org/10.1016/S0034-4257\(02\)00095-0](https://doi.org/10.1016/S0034-4257(02)00095-0)
- Hansen, M. C., Defries, R. S., Townshend, J. R. G., & Sohlberg, R. (2000). Global Land Cover Classification at 1 km Spatial Resolution Using a Classification Tree Approach. *International Journal of Remote Sensing*, 21, 1331-1364. <https://doi.org/10.1080/014311600210209>
- Haque, M. I., & Basak, R. (2017). Land Cover Change Detection Using GIS and Remote Sensing Techniques: A Spatio-Temporal Study on Tanguar Haor, Sunamganj, Bangladesh. *The Egyptian Journal of Remote Sensing and Space Sciences*, 20, 251-263. <https://doi.org/10.1016/j.ejrs.2016.12.003>
- Jin, C., Xuehong, C., Xihong, C., & Jun, C. (2010). Change Vector Analysis in Posterior Probability Space: A New Method for Land Cover Change Detection. *IEEE Geoscience and Remote Sensing Letters*, 8, 317-321. <https://doi.org/10.1109/LGRS.2010.2068537>
- Johnson, R. D., & Kasischke, E. S., (1998). Change Vector Analysis: A Technique for the Multispectral Monitoring of Land Cover and Condition. *International Journal of Remote Sensing*, 19, 411-426. <https://doi.org/10.1080/014311698216062>
- Kobayashi, T., Tateishi, R., Alsaadeh, B., Sharma, R., Wakaizumi, T., Miyamoto, D. et al. (2017). Production of Global Land Cover Data-GLCNMO2013. *Journal of Geography and Geology*, 9, 1-15. <https://doi.org/10.5539/jgg.v9n3p1>
- Loveland, T. R., Reed, B.C., Brown, J. F., Ohlen, D. O., Zhu, Z., Yang, L. et al. (2000). Development of a Global Land Cover Characteristics Database and IGBP DISCover from 1 km AVHRR Data. *International Journal of Remote Sensing*, 21, 1303-1330. <https://doi.org/10.1080/014311600210191>
- McFeeters, S. K. (1996). The Use of the Normalized Difference Water Index (NDWI) in the Delineation of Open Water Features. *International Journal of Remote Sensing*, 17, 1425-1432. <https://doi.org/10.1080/01431169608948714>
- Nackaerts, K., Vaesen, K., Muys, B., & Coppin, P. (2005). Comparative Performance of a Modified Change Vector Analysis in Forest Change Detection. *International Journal of Remote Sensing*, 26, 839-852. <https://doi.org/10.1080/0143116032000160462>
- Painter, T. H., Rittger, K., McKenzie, C., Slaughter, P., Davis, R. E., & Dozier, J. (2009). Retrieval of Subpixel Snow Covered Area, Grain Size, and Albedo from MODIS. *Remote Sensing of Environment*, 113, 868-879. <https://doi.org/10.1016/j.rse.2009.01.001>
- Rogers, A. S., & Kearney, M. S. (2004). Reducing Signature Variability in Unmixing Coastal Marsh Thematic Mapper Scenes Using Spectral Indices. *International Journal of Remote Sensing*, 25, 2317-2335. <https://doi.org/10.1080/01431160310001618103>
- Rosenthal, W., & Dozier, J. (1996). Automated Mapping of Montane Snow Cover at Subpixel Resolution from the Landsat Thematic Mapper. *Water Resources Research*, 32, 115-130. <https://doi.org/10.1029/95WR02718>
- Salomonson, V. V., & Appel, I. (2004). Estimating Fractional Snow Cover from MODIS Using the Normalized Difference Snow Index. *Remote Sensing of Environment*, 89, 351-360. <https://doi.org/10.1016/j.rse.2003.10.016>
- Sharma, R. C., Tateishi, R., & Hara, K. (2016a). A Biophysical Image Compositing Tech-

- nique for the Global-Scale Extraction and Mapping of Barren Lands. *International Journal of Geo-Information*, 5, 225. <https://doi.org/10.3390/ijgi5120225>
- Sharma, R. C., Tateishi, R., & Hara, K. (2016ab). A New Water-Resistant Snow Index for the Detection and Mapping of Snow Cover on a Global Scale. *International Journal of Remote Sensing*, 37, 2706-2723. <https://doi.org/10.1080/01431161.2016.1183832>
- Sharma, R. C., Tateishi, R., Hara, K., Gharechelou, S., & Lizuka, K. (2016). Global Mapping of Urban Built-Up Areas of Year 2014 by Combining MODIS Multispectral Data with VIIRS Nighttime Light Data. *International Journal of Digital Earth*, 9, 1004-1020. <https://doi.org/10.1080/17538947.2016.1168879>
- Tateishi, R., Hoan, N. T., Kobayashi, T., & Alsaaidh, B. (2014). Production of Global Land Cover Data-GLCNMO2008. *Journal of Geography and Geology*, 6, 99-122. <https://doi.org/10.5539/jgg.v6n3p99>
- Tateishi, R., Uriyangqai, B., Al-Bilbisi, H., & Ghar, M. A. (2011). Production of Global Land Cover Data-GLCNMO. *International Journal of Digital Earth*, 4, 22-49. <https://doi.org/10.1080/17538941003777521>
- Tucker, C. J. (1979). Red and Photographic Infrared Linear Combinations for Monitoring Vegetation. *Remote Sensing of Environment*, 8, 127-150. [https://doi.org/10.1016/0034-4257\(79\)90013-0](https://doi.org/10.1016/0034-4257(79)90013-0)
- Zha, Y., Gao, J., & Ni, S. (2003). Use of Normalized Difference Built-up Index in Automatically Mapping Urban Areas from TM Imagery. *International Journal of Remote Sensing*, 24, 583-594. <https://doi.org/10.1080/01431160304987>